RESEARCH ARTICLE

Key Points:

- In tidal systems, *Pinna nobilis* distribution is strongly affected by the bottom topography and the duration and frequency of emersion
- There is a significant positive correlation between the density of *P. nobilis* and seagrass cover
- Summer time monitoring of *P. nobilis* using unmanned aerial vehicles (UAVs) is not effective when the tidal flats are emerged and seagrass leaves obscure the shells

Supporting Information:

Supporting Information may be found in the online version of this article.

Correspondence to::

S. Silvestri,
sonia.silvestri5@unibo.it

Author Contributions:

Conceptualization: Sonia Silvestri
Data curation: Sonia Silvestri, Veronica Capra, Sara Cucchiaro
Formal analysis: Sonia Silvestri, Veronica Capra
Investigation: Sonia Silvestri, Veronica Capra, Sara Cucchiaro
Methodology: Sonia Silvestri
Resources: Sonia Silvestri, Sara Cucchiaro, Paolo Tarolli
Supervision: Sonia Silvestri
Validation: Sonia Silvestri, Veronica Capra, Mattia Pivato, Paolo Tarolli

Tides, Topography, and Seagrass Cover Controls on the Spatial Distribution of *Pinna nobilis* on a Coastal Lagoon Tidal Flat

Sonia Silvestri[1] [iD], **Veronica Capra[1], Sara Cucchiaro[2,3]** [iD], **Mattia Pivato[4]** [iD], **and Paolo Tarolli[2]** [iD]

[1]Department of Biological Geological and Environmental Sciences, University of Bologna, Bologna, Italy, [2]Department of Land, Environment, Agriculture and Forestry, University of Padova, Padova, Italy, [3]Department of Agricultural, Food, Environmental and Animal Sciences, University of Udine, Udine, Italy, [4]Department of Civil, Environmental and Architectural Engineering, University of Padova, Padova, Italy

Abstract In the last two decades *Pinna nobilis*, the largest bivalve mollusk endemic to the Mediterranean Sea, has recolonized the tidal flats of some coastal lagoons along the Italian Adriatic coast. In this study, we investigate the influence of tides on the spatial distribution and density of a *P. nobilis* population developing on a tidal flat of the Venice lagoon (NE Italy) by exploiting remote sensing technologies. Our results show that there is a threshold topographic elevation (about 0.5 m below mean sea level for the studied tidal flat) above which the number and duration of emersions become limiting factors of *P. nobilis* abundance. Above this elevation, the population density decreases sharply. Densely populated areas tend to occur in tidal flat depressions, where the duration and frequency of emersions are low. We find, however, that the population density has large spatial variability in response to other factors, such as the seagrass percentage cover. The density of the shells increases with increasing seagrass percentage cover, and the dense *P. nobilis* population ($0.8–2.68$ N/m^2) grows within the *Cymodocea nodosa* meadow that has a high seagrass percentage cover (>85%). However, within the seagrass meadow with the highest percentage cover, the bivalve preferentially colonizes the portion closest to the main channel, a possible source of nutrients. The shift to *C. nodosa*—dominated meadows in the Venice lagoon occurred during the last two decades has probably facilitated the observed colonization by *P. nobilis*. Our findings provide management information for protection and/or restoration of *P. nobilis* in coastal lagoons.

Plain Language Summary *Pinna nobilis* is the largest mollusk of the Mediterranean Sea and strictly protected by European laws. Recently this species has been attacked by pathogens which are causing mass mortality events. In early 2021, the *P. nobilis* population of the Venice lagoon (Italy) was attacked and is in risk of disappearing. Thanks to a survey performed using a drone in the summer of 2020, we studied the pre-epidemic distribution of the *P. nobilis* population colonizing a tidal flat. We found that exposure to limited emersions is a key factor for the bivalve survival as emersions can cause desiccation. Another key factor is the seagrass percentage cover: *P. nobilis* tends to colonize dense portions of the seagrass meadows, often close to the channels, which are a potential source of food. Until early 2021, when the pathogens attacked, the population growth has been likely facilitated by a constant expansion of *Cymodocea nodosa*, a subtropical seagrass species. The expansion of *C. nodosa* has probably been promoted by a small but constant increase of the water temperature during the last two decades. Our findings provide management information for the protection and/or restoration of *P. nobilis* in coastal lagoons.

1. Introduction

Pinna nobilis (Linneaus 1758), commonly known by the name of "noble pen shell" or "fan mussel," is the largest bivalve mollusk in the Mediterranean, where it has been present since the end of the Miocene (Gómez-Alba, 1988). Its large valves can exceed 100 cm in length (García-March & Vicente, 2006; García-March et al., 2002), and some individuals can reach 45 years of age (Rouanet et al., 2015).

In the last two decades the population of *P. nobilis* has recolonized some lagoons along the Italian coast of the Adriatic Sea (Curiel et al., 2020; Marrocco et al., 2018; Russo, 2012), where the fan mussel disappeared in the 20th century. As reported by Russo (2012), in 2006/2007 a significant population of *P. nobilis* was observed in certain areas of the Venice lagoon (NE Italy) with a density of up to 12–16 individuals/m^2 (Russo, 2012). Since

Writing – original draft: Sonia Silvestri
Writing – review & editing: Sonia Silvestri, Veronica Capra, Sara Cucchiaro, Mattia Pivato, Paolo Tarolli

then, *P. nobilis* has colonized several areas in the central and southern basins of the lagoon, and there are now hundreds of individuals that inhabit the vegetated tidal flats. Even though *P. nobilis* is known for its ability to colonize open sea floor areas of up to 60 m in depth when turbidity is low (Marrocco et al., 2019), its presence in estuaries and lagoons is not rare (García-March et al., 2020). In such environments the individuals grow fast, due to eutrophic conditions characterized by typically high concentrations of nitrates, ammonium, and phosphorus, that in turn increase the availability of phytoplankton and zooplankton. In lagoons, however, individuals show lower longevity than in open sea conditions (García-March et al., 2020). These findings confirm a previous study by Alomar et al. (2015) that reports that eutrophic environments increase individuals' growth rate and yet decrease their survival rate with respect to oligotrophic conditions.

Besides nutrient loading, there are several geophysical and biogeochemical variables that influence the survival of *P. nobilis*. Among them, favorable hydrodynamic conditions are a key factor in the colonization of lagoons, since in these environments *P. nobilis* rarely experience high water velocities that may prove harmful to them (García-March et al., 2020). In fact, the survival of the mollusk depends on its ability to anchor through the byssus filaments to sediments such as stones, sand, rhizomes of marine phanerogams, bio-detrital fragments, and roots. Strong hydrodynamic forces put the stability of the mollusk at risk (García-March et al., 2007). Therefore, shallow lagoon waters, where tidal flats and channels are sheltered by the presence of barrier islands and salt marshes, are an ideal environment for *P. nobilis* development.

Hydrodynamic forces appear to also influence the orientation of the shells. In open sea environments, this factor influences the size and spatial distribution of individuals, and their growth rate (García-March et al., 2007). A common shell orientation within a population may be linked to the survival of only those individuals that are exposed to lower drag forces (García-March et al., 2007). However, another possible explanation may be linked to food availability. In fact, microtopography effects on currents and resuspension may influence the orientation of shells, favoring the food intake of individuals that open their shells toward the current (Addis et al., 2009; Coppa et al., 2019).

An important factor influencing hydrodynamics is the presence of seagrass meadows in the areas where *P. nobilis* develops. The mollusk is often found within seagrass meadows and favors those composed by *Posidonia oceanica* or *Cymodocea nodosa* (Zavodnik et al., 1991). Seagrass leaves (a) perform the important task of attenuating the hydrodynamic stress (Hendriks et al., 2011; Manca et al., 2012), (b) provide protection from predators especially for young organisms and facilitate the settlement of the larvae (Hendriks et al., 2008). Seagrass meadows, however, trap suspended sediments and nutrients (Folkard, 2005; McGlathery et al., 2007) and prevent the resuspension of sediments from the bottom (Carniello et al., 2014; Moriarty & Boon, 1989). Thus, a dense seagrass population may interfere with the feeding needs of *P. nobilis*. There is, therefore, a trade-off between the advantage of being protected by the seagrass leaves and the disadvantage that the dense plant population may interfere with the filtering activity. In fact, *P. nobilis* has been found to mainly colonize the edges of seagrass meadows, where individuals can maximize the filtering action while maintaining the advantage of being protected by the plants (Coppa et al., 2013, 2019; Koch et al., 2006; Manca, 2010).

In addition to hydrodynamics, other environmental forcings can change the equilibrium and influence the development of seagrasses and consequently of the *P. nobilis* populations that develop within these meadows. One example is water temperature, which plays an important role in controlling site specific seasonal seagrass growth (Lee et al., 2007) and in lagoons and estuaries may influence the optimal depth at which seagrass populations grow (Carr et al., 2010). Generally, the optimal growth temperature for temperate species ranges between 11.5 and 26 °C (Lee et al., 2007). However, different species may prefer more limited temperature ranges and have different optimal temperatures. For example, the growth of *C. nodosa* is stimulated by higher temperature, with an optimal temperature of 24.5 °C. In fact, this species is included among the subtropical species (Lee et al., 2007). On the contrary, *Zostera marina*, a typical temperate species, has its optimal growth temperature at around 15 °C (Lee et al., 2007).

Although, as we have seen, there has been ample interest in the effects of hydrodynamics on *P. nobilis*, and in particular the dragging forces, one aspect linked to hydrodynamics has been completely neglected: tidal oscillations. Such an aspect is of key importance in coastal tidal systems such as lagoons and estuaries. In these systems, different portions of the basins are subject to different flooding periods and frequencies, depending on the bottom topography and the characteristics of the tidal wave. During propagation within shallow coastal basins, the tidal

wave is modified by the interaction with the bottom: while channels provide preferential paths for tide propagation, tidal flats and salt marshes attenuate the tide (i.e., reduce its amplitude), also creating a phase time-lag (e.g., Friedrichs & Aubrey, 1988). The typical nonlinearity of such tidal modifications produces high spatial variability in the time and frequency with which tidal flats and marshes are flooded or emerged (Silvestri et al., 2018). Despite the importance of tides for tidal systems, we could not find any papers specifically investigating the interaction between bottom geomorphology, tidal oscillation, and the colonization and survival of the *P. nobilis* population, which leaves a number of open questions. The purpose of this study is to investigate if there are specific patterns in the distribution of *P. nobilis* over a tidal flat in relation to its geomorphology and the seagrass vegetation percentage cover, defined as the percentage of the ground surface covered by vegetation. In estuaries and lagoon systems, tidal flats are often emerged exposing *P. nobilis* individuals to possible desiccation (Prado et al., 2020). Emersion times may be a strong limiting factor to the development of *P. nobilis* populations; hence, we analyze the frequency of emersions and the total emersion time during the year and in different seasons. The correlation between the density of individuals (i.e., the number of individuals per unit area) and the seagrass percentage cover is also investigated, as well as other environmental forcings. Our results contribute to detect some of the main geomorphological and environmental factors that likely drove the population growth in the last 15 years and provide management information for protection and/or restoration methods. *P. nobilis*, is a protected species under the European Council Directive 92/43/EEC since 1992 and has been recently listed as Critically Endangered on the IUCN Red List of Threatened Species (Kersting et al., 2019) due to pathogens that are causing mass mortality events across the entire Mediterranean region (Carella et al., 2019, 2020). Recent surveys report that during the first months of 2021 the *Haplosporidium pinnae* pathogen has attacked several individuals of *P. nobilis* within the Venice lagoon (http://www.ismar.cnr.it/eventi-e-notizie/notizie/pinna-nobilis-si-aggrava-le-mergenza) causing their death. Therefore, our study, based on a survey performed in June 2020, can be considered as a pre-epidemic reference to detect how bottom topography, emersion frequencies, and duration control the spatial distribution of *P. nobilis* on the studied tidal flat. Our findings can contribute to study, preserve, and eventually restore the *P. nobilis* population within the Venice lagoon and in other lagoon environments across the Mediterranean region. In other sites, in fact, restoration efforts have already started, involving larval dispersal from sites unaffected by pathogens and recolonization through recruitment of resistant juveniles (Kersting et al., 2020). Other examples of effective restoration activities are reported in literature and involve transplantation of individuals of different sizes (García-March & Vicente, 2006; Trigos and Vicente, 2016). To maximize the effectiveness of transplantation efforts, at least for lagoon environments, the knowledge of the geomorphic controls that leaded to pre-epidemic *P. nobilis* spatial distributions is of key importance and may contribute to increase the likelihood of survival of transplanted individuals.

2. Study Site

We selected a tidal flat colonized by *P. nobilis* located within the Venice lagoon (NE Italy). With an area of about 550 km^2, the Venice lagoon is the largest lagoon of the Mediterranean Sea. The lagoon is separated from the north Adriatic Sea by two barrier islands and is connected to the sea by three inlets (Figure 1) that serve four subbasins. The Venice lagoon is characterized by an average depth of about 1.5 m and a microtidal tidal regime with maximum tidal excursion of about ±70 cm around mean sea level at the inlets.

The study site is located within the central subbasin near the Malamocco inlet (Figure 1), where a population of *P. nobilis* composed of just a few individuals was first detected in 2006/2007 and has increased over time (Russo, 2012). Even though there are no studies that determine the precise size of the population, Russo (2012) documented densities of up to 16 individuals per square meter. The mudflat selected for this study is delimited in all directions by small to large channels. Two very small channels to the North and to the East separate the mudflat from Pellestrina island. The channel to the South is a minor channel that has a very limited boat traffic, while the large channel to the West is the major channel with considerable boat traffic as it connects the Pellestrina town to the inlet and the city of Venice.

The mudflat has an extent of about 28,470 m^2 and is partially covered by a seagrass meadow of *C. nodosa* and *Zostera noltii* (with an extremely limited presence of *Z. marina* along the south channel). Records and maps (Atlante della Laguna, 2021; SOLVe, 2021) report that both species were already present in 2002; however, at that time, the population was mixed and the portion of the tidal flat covered by seagrasses was smaller (Figure S1 in Supporting Information S1). Both the cover extent and the density of the two species have increased over
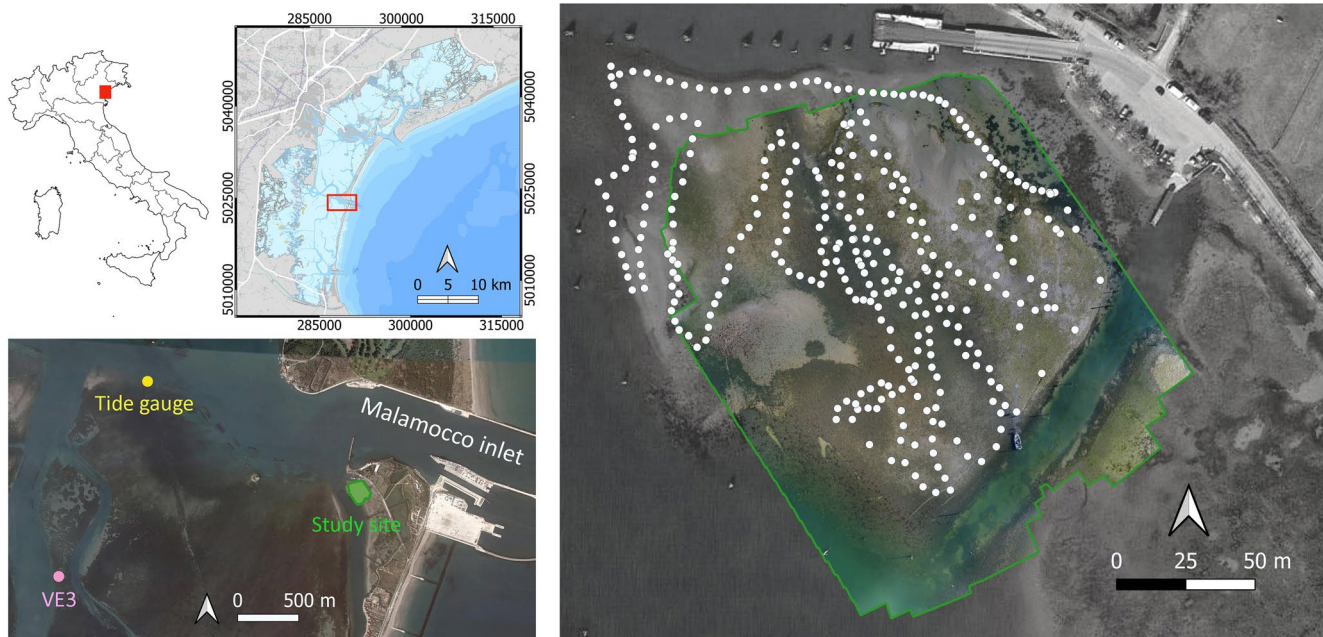
Figure 1. The study site within the Venice lagoon (Italy; coordinates shown in the map: UTM33N WGS84). The location of the tide gauge "Malamocco Porto" (yellow point), the multiparametric probe "VE3" (pink point), and the study site (green polygon) are visible in the bottom-left figure. The figure to the right zooms on the study site showing the ortho-photo mosaic overlaid on the Google Satellite base map (provided by QGIS). White points indicate the Global Navigation Satellite System (GNSS) measurements.

time (see Table S1 in Supporting Information S1). This is consistent with the information available from the entire central and south basins of the Venice lagoon, where tidal flats are mainly covered by seagrass meadows, and we find specifically the three species *C. nodosa*, *Z. marina*, and *Z. noltii*. Nowadays the meadows are mainly composed by monospecific patches, even though mixed patches can be found far from the inlets (Figure S2 in Supporting Information S1). The composition of seagrass meadows has changed over time, shifting in the period 2002–2017 from a multispecies population to an almost monospecific one, dominated by *C. nodosa* (Figure S2 in Supporting Information S1), a species that is still the most abundant across the tidal flats (Atlante della Laguna, 2021; SOLVe, 2021). Both the seagrass cover extent and density have also increased over time across the central and south basins (Table S2 in Supporting Information S1).

The expansion of *C. nodosa* can probably be ascribed to favorable conditions such as a constant increase in water temperature as will be further discussed below.

It is interesting to note that in the studied mudflat *C. nodosa* and *Z. noltii* cover two separate portions, with *C. nodosa* colonizing the half to the West and *Z. noltii* the half to the East (Figure S1 in Supporting Information S1).

3. Methods

3.1. Unmanned Aerial Vehicle and GNSS Surveys

On the 23 June 2020 at 06:05 a.m. (GMT; 07:05 solar local time) unmanned aerial vehicle (UAV) images were collected at low tide with a DJI Zenmuse X4S camera (20 Mpixels, focal length 8.8 mm, 1-inch CMOS Sensor) mounted on a professional quadcopter DJI Matrice210v2. At the time of the flight, about half of the tidal flat was flooded while half was above the water level. The drone flight was planned to provide a side overlap of 70% and a front overlap of 85% among pictures, which is essential for the image matching algorithms used in Structure from Motion (SfM) photogrammetric technique (Carrivick et al., 2016). In order to ensure such overlap as well as a high resolution (image footprint with a Ground Sampling Distance-GSD, i.e., distance between two consecutive pixel centers measured on the ground, of 0.008 m), the flight altitude was ~30 m. A total of 228 images were collected and the Agisoft Metashape Pro v 1.6.2 software was then used to produce an ortho-photo mosaic at 0.01-m resolution (i.e., pixels of 1 cm × 1 cm) through SfM technique. Before the acquisition of the

images, 18 Ground Control Points (GCP) were selected across the emerged portion of the tidal flat, retrieving the coordinates with a Geomax Zenith40 Global Navigation Satellite System (GNSS) in Real-Time Kinematic (RTK) mode. The planimetric positional accuracy (RMSE) of the GNSS survey was 0.011 m and the vertical was 0.016 m in real-time mode. All point coordinates were referred to WGS84/UTM zone 32N (EPSG: 32632) reference system. Two-thirds of the GCP were used in the orthorectification process while the remaining one-third of the GCP were used afterward as Check Points (CP). This step was essential to georeference the SfM ortho-photo mosaic and evaluate the photogrammetric errors (James et al., 2019). The assessment of the SfM process uncertainty was evaluated on GCPs and CPs, considering the residuals of each point (i.e., the difference between the real coordinates of this point measured with the GNSS in the field and the modeled SfM values). The $RMSE_{3D}$ (3D Root-Mean-Square Error; Remondino et al., 2017) of GCPs and CPs computed along the x, y, and z directions are 0.118 and 0.554 m, respectively. The mean of the residuals provides an indication of the accuracy of the registration process (0.031, 0.030, and 0.089 m for x, y, and z components) and the point cloud/ortho-photo mosaic (0.037, 0.039, and 0.481 m for x, y, and z components) when the GCP and CP residuals are considered, respectively. Instead, the standard deviation (StDev) of the CP residuals yields (0.027, 0.031, and 0.226 m for x, y, and z components) is an indication of the precision (Cucchiaro et al., 2018). We underline that the GCPs were placed exclusively on the emerged mudflat portion; hence, the elevation of the submersed area (which is the area of interest in this study) could not be determined due to the presence of water. For this reason, in order to retrieve the Digital Elevation Model (DEM) of the entire mudflat, we performed a second GNSS RTK survey on 26 February 2021, during a pronounced low tide that left the entire tidal flat exposed. During this second survey, a total of 313 measurements were recorded with a Topcon Hyper V GNSS system (planimetric positional accuracy around 0.017 m; vertical uncertainties around 0.024 m in real-time). The geographic coordinates were converted into WGS84 UTM 32N using the CONVERGO model provided by CISIS (Centro Interregionale per i Sistemi Informatici, geografici, Statistici). All the 331 points were then used to calculate the variogram and perform an ordinary kriging, as explained below.

3.2. Water Quality Parameters

Data collected in the period 2003–2020 with a multiparametric probe located 2.5 km away from the study site (Figure 1; probe VE3: latitude = 45.32556796 N; longitude = 12.28574527 E) were analyzed (data provided by the Ministero delle Infrastrutture e dei Trasporti—Provveditorato Interregionale alle OO.PP. del Veneto-Trentino Alto Adige-Friuli Venezia Giulia). The study site and the multiparametric probe VE3 are located within the Malamocco subbasin, central lagoon (Cucco & Umgiesser, 2006; D'Alpaos, 2010; Matticchio et al., 2017; Viero & Defina, 2016). Together with the Chioggia subbasin (southern subbasin), the Malamocco subbasin is characterized by the greatest depths in the Lagoon, and thus by limited effects on tidal propagation (Carniello et al., 2009). Given the proximity to the Malamocco inlet, the amplitude, and phase differences of the tidal oscillation at the study site and at the multiparametric probe are negligible. Moreover, the two sites are within the same physically homogeneous area for hydrodynamic aspects (Solidoro et al., 2004a) and for other water quality parameters such as water temperature, salinity, chlorophyll-a concentrations, etc. (Ghezzo et al., 2011; Solidoro et al., 2004b). Observations and models described in Solidoro et al. (2004a, 2004b) confirm that long-term observations of water quality performed by the probe VE3 can be reliably used to study the tidal flat selected for our study. Data were collected with a half-hourly temporal resolution, and daily mean, maximum, and minimum values were analyzed. Temperature, oxygen concentration, salinity, conductivity, and pH were measured by an Idronaut OCEAN SEVEN 316 multiparametric probe. Water turbidity is measured through a backscattering optical probe (Seapoint turbidity meter, operating at 880 nm), and is expressed in Formazine Turbidity Units (FTU), which is directly related to the suspended sediment concentration (Old et al., 2001). Chlorophyll concentration was measured with a Seapoint Chlorophyll Fluorometer. Finally, wind speed measurements recorded hourly at the station "Stazione Malamocco Porto" by the Venice municipality (see Figure 1; latitude = 45.339883 N; longitude = 12.295017 E; https://www.comune.venezia.it/it/archivio/1653) were used to calculate yearly averaged wind speed from 2004 to 2019.

3.3. Digital Elevation Model of the Tidal Flat, Emersion Times, and Frequencies

The 331 GNSS points were used in SAGA GIS to perform an ordinary kriging, which allowed us to infer the mudflat DEM at 1-m spatial resolution. We fitted a linear variogram model with no nugget in the 0–37-m distance

range. In order to calculate the accuracy of our results, we performed a leave-one-out analysis that yielded an RMSE just under 0.05 m. Once the error StDev across the map was calculated, we clipped the borders where the StDev values were higher than 0.08 m in order to retain only bottom elevation estimates characterized by high estimation accuracy.

Water levels in the Venice lagoon are measured every 10 min by a network of 14 tide gauges managed by the Venice municipality. After data checking, the municipality makes hourly data publicly available through their website (https://www.comune.venezia.it/it/archivio/1653). Tidal levels refer to a local datum which is anchored to a benchmark located downtown, at Punta della Salute, defined as ZMPS (https://www.comune.venezia.it/it/content/riferimenti-altimetrici). The ZMPS was referred to the Italian unique zero benchmark, which was established by measuring the sea level in the period 1937–1946 by the Italian "Istituto Geografico Militare" (IGM) in Genova (Hayford Ellipsoid oriented at Roma Monte Mario; Datum: Roma40) and then connected to the Venice ZMPS in 1968 through altimetric triangulations (Ferla et al., 2006). Specifically, at that time, there was a difference of 23.56 cm between the Genova and the Venice benchmarks. Unfortunately, the ZMPS elevation is not constant in time due to natural and human-induced subsidence. Specifically, based on several studies (Carbognin et al., 2004; Ferla et al., 2006; Tosi et al., 2013; Trincardi et al., 2016), it is found that only a natural subsidence of 0.5 mm/y affected the Venice benchmark after 1968 (i.e., no anthropogenic subsidence), for a total of 2.5 cm to be added to the 23.56 cm difference measured in 1968 (Da Lio et al., 2017; Ferla et al., 2006). Therefore, a total difference of 26.06 cm has been subtracted to the tide-gauge sea-level measurements in order to account for the difference with the national benchmark and for the subsidence experienced by the ZMPS datum.

As for the selection of the most appropriate tide gauge among all those available, the sea level at our study site is considered equivalent (i.e., same level and synchronous) to the level measured at the "Stazione Malamocco Porto" (see Figure 1; latitude = 45.339883 N; longitude = 12.295017 E). The correspondence has been checked on 2019 data using the finite-element hydrodynamic model developed by D'Alpaos and Defina (2007), finding a mean difference of 1.6 cm between the levels measured at "Stazione Malamocco Porto" and those simulated for the study site. Given such a close correspondence, we decided to use for our analyses the levels measured at "Stazione Malamocco Porto" instead of the simulated values.

Water levels recorded in 2019 were used to determine the amount of time that the surface is emerged during a year as well as the number of times the emersions occur. The calculated emersion times and frequencies were combined with the topography of the studied tidal flat to produce the corresponding maps and statistics. We used 2019 data instead of 2020 because in October–December 2020 the Mo.S.E. system became operational (Mo.S.E. stands for "Modulo Sperimentale Elettromeccanico," i.e., Experimental Electromechanical Module, the gates that prevent high tide in the lagoon during extreme surge events); hence, the measurements of the 2020 tidal levels are affected by the closures and are not representative of the submergence regime experienced by the *P. nobilis* population in the past. We exclusively used water levels recorded in 2019 to be consistent with the fact that the spatial distribution of *P. nobilis* shells and the topographic data were recorded one single time, in June 2020 and in February 2021, respectively. Therefore, considering that the topography of the tidal flat may have changed overtime, we limited our analysis to the water levels recorded in the prior year. However, for completeness, we show in Figure S3 in Supporting Information S1 that the variation of the mean tide levels calculated in the period 2005–2020 is negligible, with an annual variation of 0–0.1 m above mean sea level.

The number of emersions of the tidal flat in 2019 and the total emersion time (sum of the time of each emersion occurred in 2019) were calculated every 5 cm of depth, between −0.80 and −0.10 m. A fourth-order polynomial function was then fitted in order to assign the number of emersions and the emersion time corresponding to each pixel of the DEM.

3.4. Detection of *P. nobilis* Individuals and Seagrass Cover Assessment

Visual inspection of the ortho-photo mosaic showed that in the emerged portion of the tidal flat the seagrass partially or completely covers most of the *P. nobilis* individuals, preventing an accurate assessment of the bivalve presence. On the contrary, individuals are clearly detectable in the submerged areas (see Figure S4 in Supporting Information S1) and, since we could calculate the GSD value (i.e., GSD = 1 cm), we can estimate the size of the smallest detectable object in the image. Specifically, the Nyquist Sampling Criteria dictates that the pixel size of an image must be at least 2.3 times smaller than the object that is being resolved, and 2.8 times smaller to be safe

(Pawley, 2006). A similar approach has been successfully tested in other contexts, e.g., landslide feature automatic detection (Tarolli et al., 2012) and ditches detection (Cucchiaro et al., 2021). Applying this criterion to our ortho-photo mosaic, we estimate that the smallest detectable shell in our ortho-photo had a maximum shell width of 3 pixels, i.e., 3 cm. Considering the possible uncertainties related to other factors (i.e., the optics of the camera, slight changes in the drone altitude, distortions during the orthorectification process, etc.) we prefer to use an even more conservative criterion, hence considering a pixel 5 times smaller than the smallest detectable object. Thus, estimating that the minimum detected shell width is 5 cm. According to measurements performed by Alomar et al. (2015) in eutrophic environments and to the growth models developed by García-March et al. (2020), we speculate that the method allows us to detect individuals that are at least 1 year of age and older. Even though the visual interpretation of ortho-photos is a common process widely applied in photogrammetry, we note that the presence of seagrass may interfere with the visual detection process, especially for smaller shells and during the summer season, resulting in an underestimation of the number of small shells with respect to larger shells. Moreover, we underline that the method does not allow the operator to distinguish between alive and dead individuals, so all standing shells were visually recognized and recorded.

On the ortho-photo mosaic, we first detected the line that separates the emerged from the submerged portion of the mudflat and excluded the emerged portion from our analyses. A 5 m × 5 m grid was overlaid on the ortho-photo mosaic in the submerged area using QGIS software (Figure S5 in Supporting Information S1). The cells that entirely or partially fell outside the ortho-photo mosaic were discarded from the analysis, as well as cells where the certain recognition of individuals was prevented by the presence of rocks or artifacts. A total of 484 cells were retained. For each 25 m² cell, we determined, through visual inspection, the number of *P. nobilis* individuals, and calculated the density as number N per m² (i.e., N/m²).

Seagrass percentage cover was evaluated in two steps. An initial evaluation was performed based on the visual assessment of the seagrass distribution across of the entire mudflat, assigning each 25 m² cell to one of the four following cover classes: (a) high-cover, where plants fully cover the sediment, (b) low cover, where a mixture of plants and sediment was detectable, (c) sparse vegetation where sparse plants could be detected over a bare sediment background, and (d) bare sediment (see Figure S6 in Supporting Information S1). The high spatial resolution of the ortho-photo mosaic allowed a clear assignment of each pixel to one of the four classes by the operator also thanks to the homogeneity of the vegetation cover within each grid element. We subsequently assigned a quantitative range of vegetation percentage cover to each class by randomly selecting 10% of the 25 m² cells. A 1 m × 1 m grid was then defined within each selected cell thus obtaining 25 subcells of 1 m² (Figure S5 in Supporting Information S1). Finally, we determined the proportion of gridline intersections falling on vegetated versus nonvegetated points. This provided an estimate of the percentage cover class within the selected 25 m² cells. Specifically, we found that the high-cover class corresponds to a percentage cover range of 85–100% (i.e., 85–100% of the gridline intersections falling on vegetated pixels); the low cover class corresponds to a percentage cover in the 40–85% range; the sparse vegetation class corresponds to a 10–40% percentage cover; bare sediment corresponds to a percentage cover <10%. The correlation between the *P. nobilis* density and the seagrass percentage cover was performed using the mean percentage cover of each class (i.e., 0.93 = high-cover; 0.63 = low cover; 0.25 = sparse vegetation; 0.05 = bare sediment).

The correlation between the *P. nobilis* density and the mudflat elevation was performed based on the average elevation values calculated for the 25 m² cells falling within the DEM. A multiple regression analysis was also performed considering both the mudflat average elevation of the 25 m² cells and the seagrass percentage cover determined for the cells as independent variables. The number of emersions/yr and the emersion time (hr/yr) were calculated using the fourth-order polynomial functions retrieved as explained above and then correlated to the number of *P. nobilis* individuals. Finally, we calculated the probability density function (PDF) for different classes of emersions.

4. Results

The distribution of *P. nobilis* shells across the studied tidal flat is shown in Figure 2a. The blue line separates submerged area from the emerged area, which are the west and the east portions, respectively. The very high spatial resolution of the ortho-photo mosaic allows the visual detection of the shells as well as the characterization of the distribution of the seagrass plants (see Figures S4 and S6 in Supporting Information S1). In the
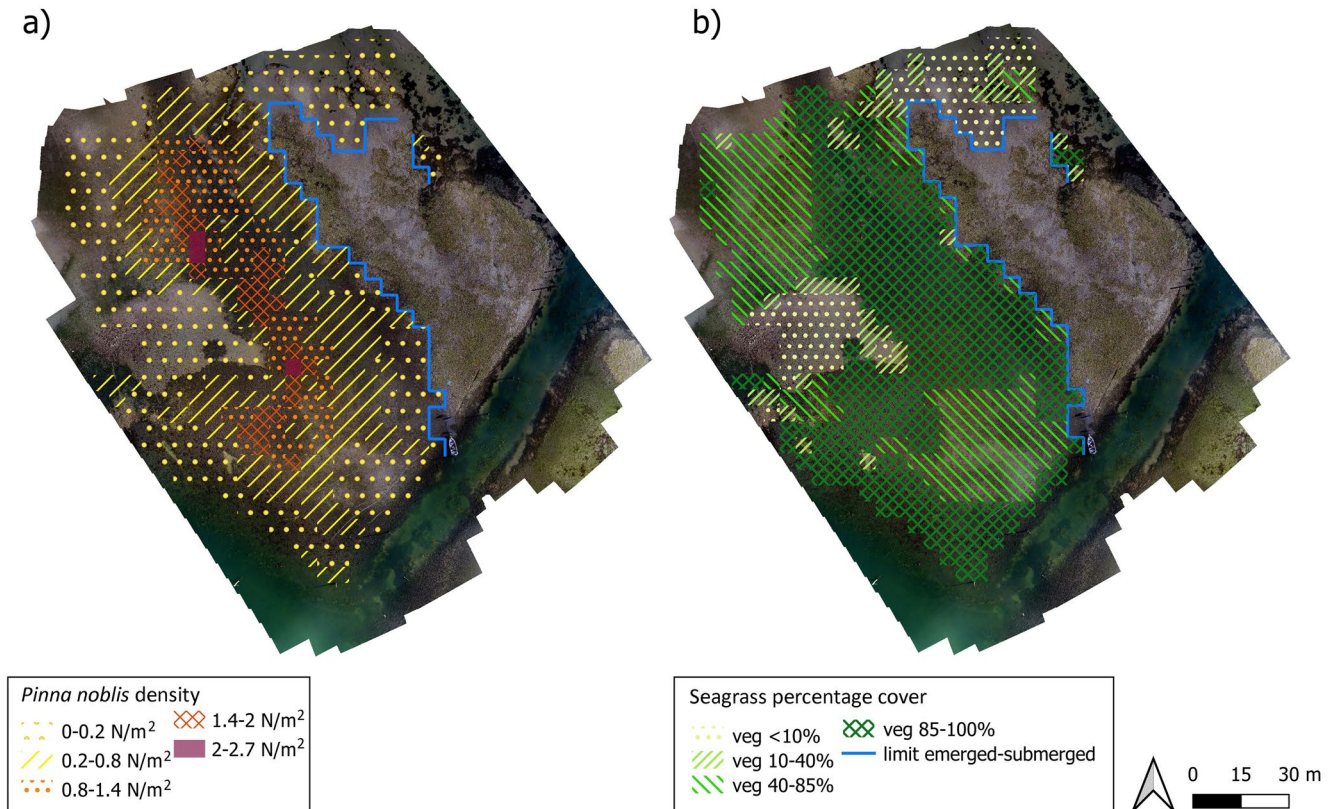
a)

b)

Pinna noblis density

- 0-0.2 N/m²
- 0.2-0.8 N/m²
- 0.8-1.4 N/m²
- 1.4-2 N/m²
- 2-2.7 N/m²

Seagrass percentage cover

- veg <10%
- veg 10-40%
- veg 40-85%
- veg 85-100%
- limit emerged-submerged

0   15   30 m

Figure 2. Distribution of *Pinna nobilis* (a) and *Cymodocea nodosa* (b) across the submerged area of the tidal flat.

submersed portion of the tidal flat, we detected 5,252 standing shells. The population has a variable density of individuals (Figure 2a): the central area is colonized by a very dense population, with up to 2.68 N/m², the shell density decreases moving away from the central part, with areas near the tidal flat boundary having densities of 0–0.2 N/m². The central portion of the mudflat appears to be also the favorite area for *C. nodosa* development (Figure 2b). The percentage cover of the meadow, in fact, is high in the central and in the south portions of the mudflat (along the main channel), while all other areas have low cover seagrass meadow or sparse plants. The two maps in Figure 2 suggest that the presence and density of *P. nobilis* is not independent of the percentage cover of *C. nodosa* even though the high density *P. nobilis* portion is smaller and concentrated in a band-shaped area that goes from NW to SE. Figure 3 also shows that the dense *P. nobilis* population grows within the high-cover

Figure 3. *Pinna nobilis* density within the four vegetation cover classes detected for *Cymodocea nodosa*. Boxes are bounded between first and third quartiles, whiskers extend to the maximum and minimum values, medians divide the boxes and crosses show the mean values.

C. nodosa meadow, and the density of the shells increases with increasing seagrass percentage cover. The ANOVA test gives a significant linear correlation (P-value < 0.01). It is interesting to note that in Figure 3 the box-plot corresponding to the high-cover seagrass meadow exhibits the highest difference between the third and the first quartiles, indicating that there is a high variability in the number of *P. nobilis* individuals that colonize this vegetation class. This is even more evident in the maps of Figure 2: even though the dense *P. nobilis* population (i.e., >0.8 N/m²) tends to colonize the *C. nodosa* high-cover class, its extent is limited to the south-west portion, and creates an elongated band-shaped structure along the edge of the meadow, while the rest of the high-cover seagrass meadow is colonized by a lower density *P. nobilis* population, with 0.2–0.8 N/m².
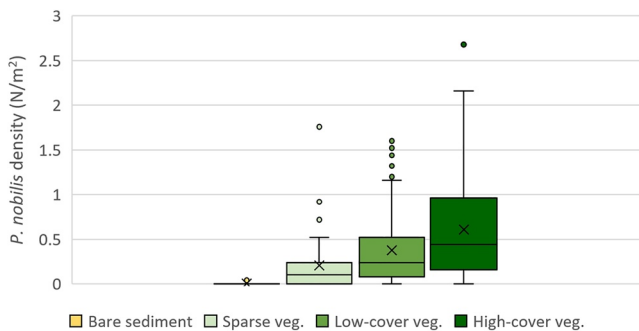
The distribution of both *P. nobilis* and *C. nodosa* suggests the possible combined influence of tidal and geomorphic factors. The mudflat, may emerge during very low tides, exposing the biota that grows on its surface to possible desiccation. In order to understand the importance of this factor for
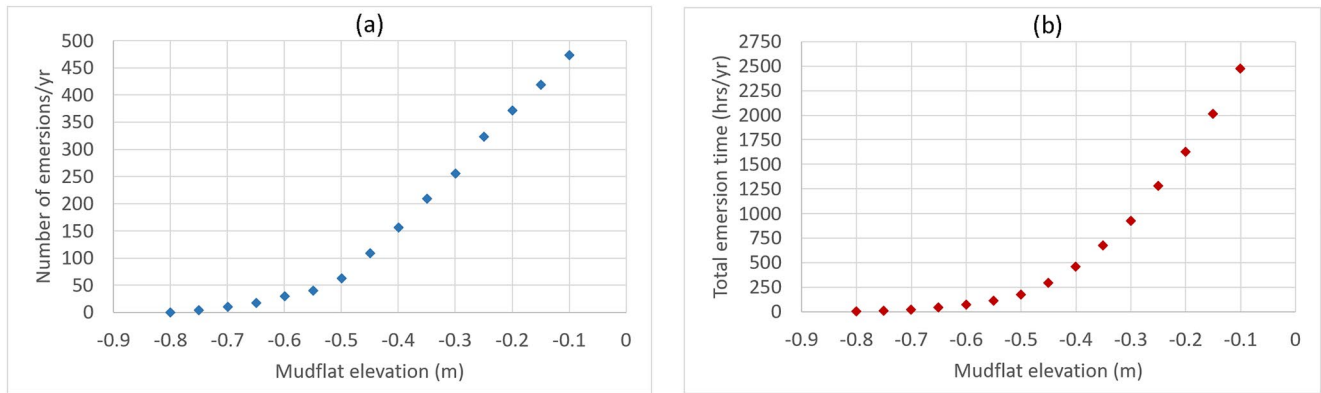
Figure 4. (a) Number of emersions in 2019 and (b) total emersion time of the mudflat during year 2019.

P. nobilis, we show in Figure 4a the number of emersions that surfaces at different elevations have experienced during 2019 at the specific study site location.

Surfaces that lie below $z = -0.8$ m never emerge, not even during extremely low tides, while the number of emersions notably increases for $z > -0.8$ m. However, this increase is nonlinear and is small for surfaces between -0.8 m $< z < -0.5$ m, while the number of emersions increases more rapidly moving from -0.5 m to higher elevations. A similar behavior is found for the number of hours in which the mudflat was emerged in 2019 (Figure 4b) and for the seasonal variation of the number of emersions (see Table S4 in Supporting Information S1), especially for the summer months when the mudflat tends to be less frequently emerged than in winter months (i.e., in January and February the Venice lagoon typically experiences the major low tides).

These results were used to compute the number of emersions and the total emersion time experienced spatially by the mudflat in 2019. In order to do this, we considered the DEM computed from kriging the 331 GNSS points collected across the tidal flat and cut based on the area surveyed with the UAV system (Figure 5a). The elevation of the tidal flat varies between $z = -0.86$ m and $z = -0.21$ m, with a depression in the central area of the permanently submersed zone. Comparing Figure 5a with the distribution of *P. nobilis* density classes (Figure 2a), we notice that shell density tends to be high within the depression, while areas with higher elevations are characterized by lower shell densities. A similar behavior can be noticed when comparing the *P. nobilis* density classes with the map of the number of emersions/year (Figure 5b). Also, in this case, the dense *P. nobilis* population tends to develop where the number of emersions is low. Finally, when comparing the distribution of the bivalve with the map of total emersion time of surfaces in 2019 (Figure 5c), we notice the same behavior.

Figure 6a shows the relation between the density of *P. nobilis* and the mudflat elevation. There is a significant linear correlation between the bivalve presence and the mudflat elevation ($R^2 = 0.50$, P-value < 0.01). When both the mudflat elevation and the seagrass density are considered as independent variables, the results of the multiple regression analysis show that R^2 increases from 0.50 to 0.52 (P-values < 0.01), suggesting that there must be other factors that influence the distribution and density of the *P. nobilis* population.

The distribution of *P. nobilis* density as a function of the number of emersions (Figure 6b) or of emersion time (Figure 6c) displays a high variability in the number of individuals that develop on the mudflat portions that experience 0–40 emersions/yr, which corresponds to the emersion time range 0–100 hr/yr. This means that in this range we find sites with both dense *P. nobilis* populations and low-density populations. On the contrary, if we examine areas of the tidal flat with $z > -0.52$ m that experience a higher number of emersions (>60 emersions/ yr) and emersion times (>142 hr/yr) we never find >0.5 N/m² (Figures 6b and 6c). The empirical PDFs of shell density (Figure 7) computed for different intervals of topographic elevation time clarify this behavior. Mudflat areas that experience <20 emersions/yr (where $z < -0.62$ m) host a large variety of possible shell density values, indicating that emersion stress is not a limiting factor in this range of elevation. Areas at higher elevations, thus experiencing higher emersion times and frequency, are associated with progressively narrower ranges of possible shell densities, indicating that where there are >60 emersions/yr (areas with $z > -0.52$ m) the emersion stress becomes the main limiting factor for *P. nobilis* development and survival.
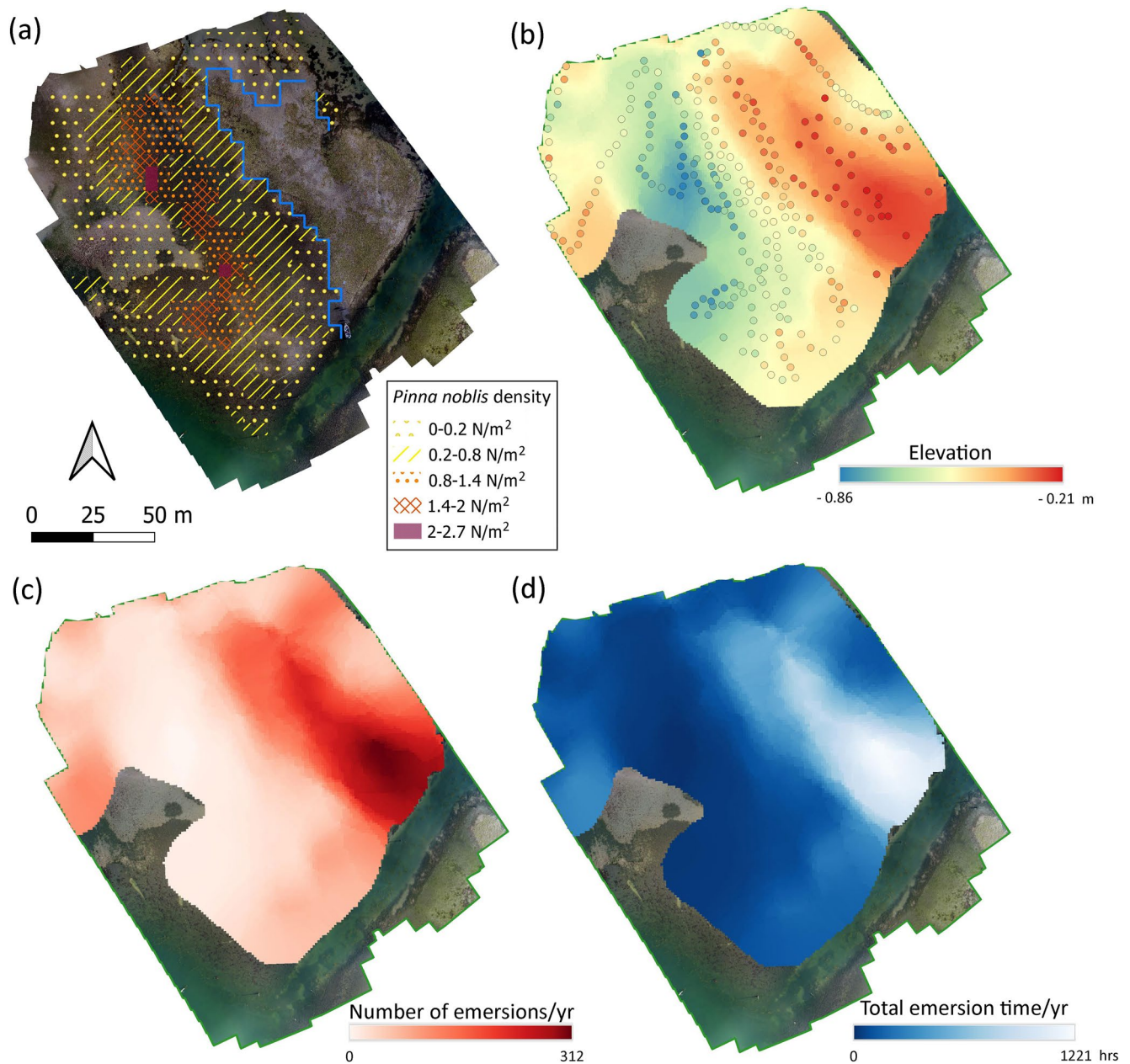
Figure 5. (a) *Pinna nobilis* density, (b) Digital Elevation Model (DEM) with the Global Navigation Satellite System (GNSS) measurements overlaid, (c) number of emersions in 2019 and (d) total emersion time in 2019.

Among the water quality parameters, water temperature records show a small but constant increase since 2003 for the daily mean values, as shown in Figure 8. The analysis of the other water quality parameters do not show particular trends for the period 2003–2020 (Figure S7 in Supporting Information S1), apart from a small decrease of suspended sediment concentrations.

5. Discussion

Coastal lagoons and estuaries across the Mediterranean host several *P. nobilis* populations and so far are the ecosystems where the species has been less attacked by harmful pathogens (García-March et al., 2020). The hydrodynamic conditions typical of Mediterranean microtidal systems are ideal for the development of young *P. nobilis* individuals, which within the quiet lagoon waters can grow protected from strong currents and extreme
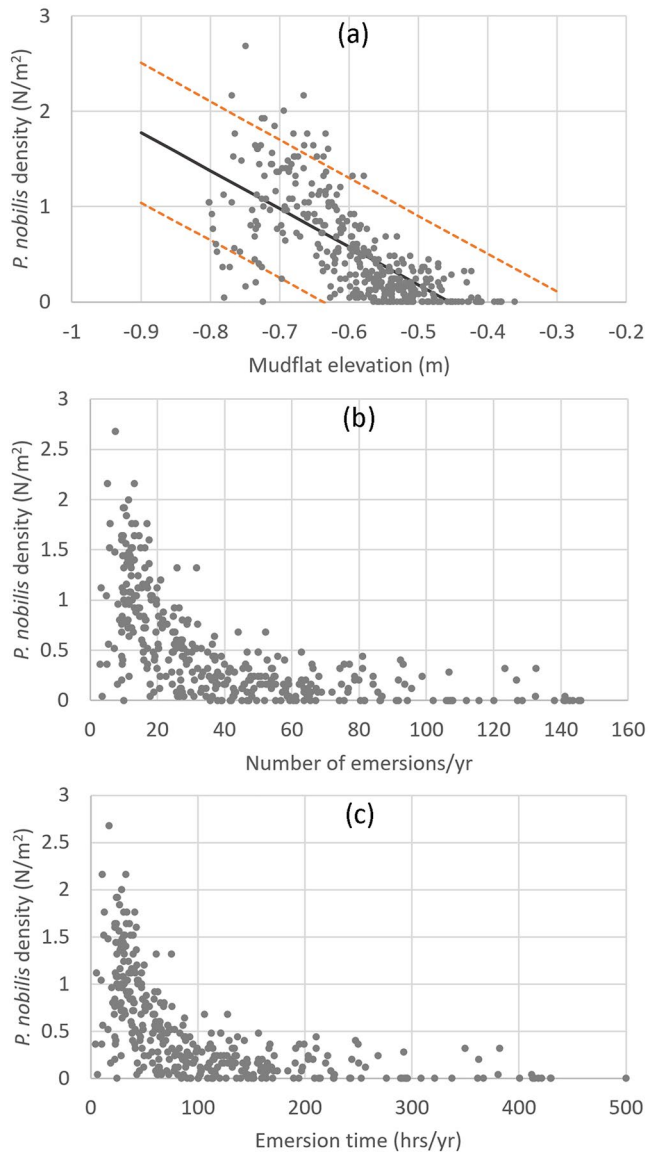
Figure 6. Relationship of *Pinna nobilis* density with (a) the elevation of the tidal flat, (b) the number of emersions in 2019, and (c) the total emersion time in 2019. The orange dashed lines in (a) is the prediction interval, i.e., the estimate of the interval in which a future observation will fall with 95% probability.

events (García-March et al., 2007, 2020). These tidal systems provide nutrients and act as nurseries (Marrocco et al., 2018). However, a number of environmental forcings typical of tidal systems appear to limit the spread of *P. nobilis* population and the growth of individuals. Among the limiting factors, the influence of the tide combined with the bottom topography is one of the most important because it regulates the frequency of emersion periods and the duration of exposure to desiccation. Our analyses show that the density of *P. nobilis* population is highly correlated to mudflat elevation (Figure 6a). This result suggests that there is a range of elevations at which *P. nobilis* preferably grows and there is a higher elevation limit to the colonization of *P. nobilis*, which is likely related to the number of emersions and the exposure time that the species can tolerate. In fact, the number of individuals decreases rapidly as the number of emersions/year (Figure 6b) and the duration of emersion periods (Figure 6c) increase. This is likely because at higher elevations the mollusk faces the risk of desiccation. Seasonality may also have an effect in terms of desiccation. This study did not explore the consequences of emersions on the physiology of individuals; however, we notice that, given a specific elevation of the tidal flat, during spring-summer months (April to September) the number of emersions is lower than in autumn/winter months (see Table S4 in Supporting Information S1). This is because at our study site major spring-tides occur between December and February. However, we suggest that air temperature and incident sunlight may be important factors in the desiccation process of the mollusk. Thus, prolonged emersions in winter may be less dangerous to *P. nobilis* individuals than in spring and summer, when higher irradiance may put at risk the survival of individuals emerged for long periods. Another important factor that may influence desiccation is the presence of seagrass. We have seen that during low tides, seagrass leaves tend to cover the mollusk preventing its identification through UAV images. This circumstance may also create a sort of favorable microclimate for the shells that are protected from the direct incidence of sunlight by being covered by leaves and are less subject to continuous shell fractures and reconstructions (Prado et al., 2021). Looking at the distribution of *P. nobilis* individuals over the mudflat we see that areas experiencing <20 emersions in a year host the majority of the population, but interestingly in these areas we can find a wide range of population densities (Figure 7). Therefore, in these areas, the number of emersions and the emersion time are not the only factors driving the distribution of *P. nobilis*. On the contrary, there must be also other factors affecting the presence and distribution of the mollusk population, as, e.g., the food availability. As we move toward shallower areas, where the emersions increase, the number of individuals quickly decreases, and we never find >0.5 N/m² in areas that experience >60 emersions in 1 year (Figure 7). The desiccation conditions related to frequent emersions are clearly the driving factor here, limiting the colonization of the bivalve.

The distribution of *P. nobilis* over the mudflat confirms our hypothesis: the large majority of the population tends to grow in the depression in the central part of the mudflat that was flooded during the UAV survey (Figure 5a), where the frequency of emersions and the total emersion time are very low (Figures 5b and 5c). Few individuals survive at higher elevations, which are characterized by complete absence of individuals over large surfaces and are often emerged (Figure 5b) for long periods (Figure 5c). Our results also suggest that *P. nobilis* individuals tend to survive at depth lower than −0.5 m. This appears also as the threshold depth at which we observe a clear change in the number of emersions (Figure 4a): the increase in the number of emersions of the mudflat with elevations between −0.8 m and −0.5 m is much lower than the increase of emersions of the surfaces higher than −0.5 m. A similar relation is evident when looking at the amount of emersion time of the mudflat with respect to increasing elevation (Figure 4b). The elevation −0.5 m corresponds to 63 emersions, for a total of 171 hr in a year
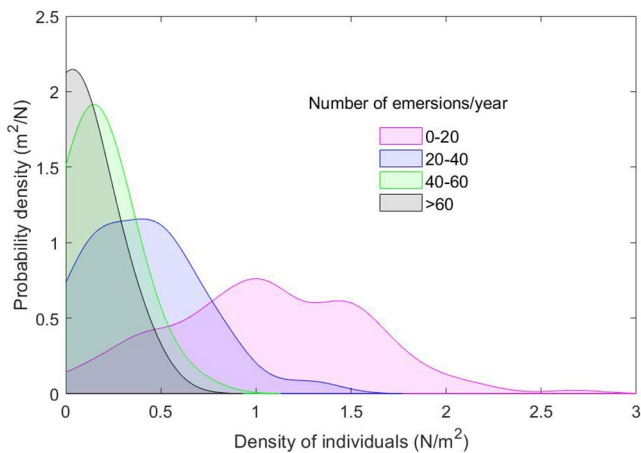
Figure 7. Empirical probability density functions (PDFs) of the density of *Pinna nobilis* individuals for different ranges of emersions/yr. The PDFs were obtained from data through Kernel Density Estimation (e.g., Bowman & Azzalini, 1997).

(Figures 4a and 4b); hence, it is in good agreement with the results obtained by calculating the PDF (Figure 7).

Our results confirm that, as in open water ecosystems, in the Venice lagoon *P. nobilis* colonizes preferably dense *C. nodosa* meadows (Figure 2), and there is a significant positive correlation between the density of shells and the seagrass percentage cover (Figure 3). We speculate that, given the absence of harmful hydrodynamic conditions in lagoon environments, one of the main reasons that lead *P. nobilis* to colonize seagrass meadows in tidal systems may be related to protection from desiccation during low tides and emersion periods. What is evident from Figure 2 is that, within the dense seagrass meadow, *P. nobilis* prefers to grow along the edge toward the main channel to the west, which is directly connected to the lagoon inlet, where nutrients are likely to be more abundant and easier to trap since the tide rises from that direction. Other studies have reported a similar pattern (Coppa et al., 2013, 2019; Koch et al., 2006; Manca, 2010), even though in open water environments, confirming the trade-off strategy between living protected by the seagrass leaves and the maximization of nutrient trapping. Even though *P. nobilis* colonizes preferably dense seagrass meadows, this does not mean that all dense seagrass meadows host *P. nobilis*. This is evident looking at the results of the multivariate analysis: the small increment of R^2 shows that the seagrass cover gives a small contribution in explaining the density of *P. nobilis* and there must be also other factors affecting the density of the bivalve, as discussed above. As previously discussed, starting in 2006/2007, *P. nobilis* has recolonized the Venice lagoon and such behavior might indicate that some environmental factors have changed during those years, favoring the spread of this bivalve. As we have shown in Figures 2 and 3, one of the main factors that created a favorable environment for *P. nobilis* has probably been the expansion of the *C. nodosa* meadow. In the last two decades, *C. nodosa* has substituted other seagrass species in the Venice lagoon, as confirmed by maps and records provided by local agencies (Figure S2 and Table S2 in Supporting Information S1). In general, the area covered by the seagrass meadows and the density of plants have increased at the lagoon scale (Figure S2 in Supporting Information S1) as well as at the study site scale (Figure S1 in Supporting Information S1). This behavior of *C. nodosa* is in line with other studies that describe it as a fast colonizer species (Cancemi et al., 2002). Being a subtropical species (Lee et al., 2007), the spread of *C. nodosa* may have been facilitated by a small but constant increase of water temperature that has been recorded by the local probe VE3 through continuous measurements performed in the last 18 years (Figure 8). *C. nodosa* has not only colonized greater surface areas but also increased the percentage cover, developing a dense meadow that now covers the large majority of the tidal flats of the southern lagoon. There has been a decrease of turbidity recorded by the local probe (Figure S7g in Supporting Information S1), especially during high resuspension events. Wind speed records do not show any specific decrease in the last 18 years (Figure S7h in Supporting Information S1), sustaining the hypothesis that another factor must have influence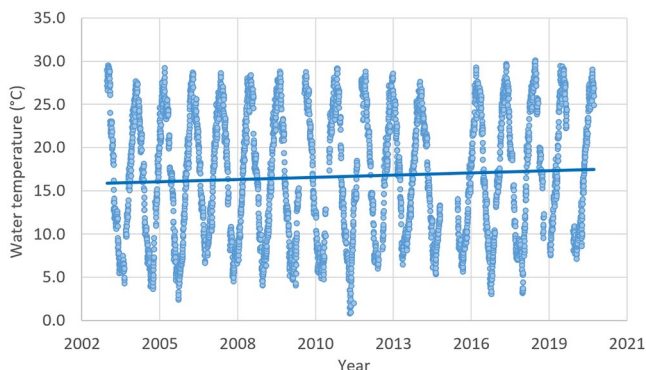d the lower maxima turbidity values recorded over time. Seagrass is known for its ability of trapping sediments and decreasing resuspension (Carniello et al., 2014; Carr et al., 2010; Folkard, 2005; McGlathery et al., 2007; Moriarty & Boon, 1989; Sfriso et al., 2005) and thus lower turbidity values confirm the presence of larger and denser *C. nodosa* meadows, as reported by maps and records (Atlante della Laguna, 2021; SOLVe, 2021). We conclude by noting that even though the constant water temperature increase may be a favorable condition for *C. nodosa*, it may become a threat for *P. nobilis* and especially for juveniles, by increasing mortality rates (Basso et al., 2015). This is not just a threat for *P. nobilis*: high summer temperatures and low food availability will probably characterize the Mediterranean Sea in the near future, bringing more frequent mass mortality events of invertebrates in general (Coma et al., 2009). Beside water temperature variations, other consequences of climate change and increasing human pressure put *P. nobilis* populations at risk since the mollusk has a strong response to geophysical and biogeochemical changes. These include

Figure 8. Mean values and linear interpolation of the water temperatures recorded daily by the multiparametric probe.

but are not limited to sea-level rise, sedimentation and erosion, pollution, invasive species, and many other factors that will particularly impact estuaries and lagoons. Even though, apart from water temperature and turbidity, no specific trends of other water quality parameters were observed in the 2003–2020 records of the multiparametric probe VE3 (see Figure S6 in Supporting Information S1), in future scenarios this could change. In fact, the data and the observations presented in this study have been collected before the Mo.S.E. system became operational; therefore, the impact of the gates has not been assessed. The closures of the Mo.S.E. system may alter the emersion frequencies and duration of the studied area. However, the gates are operated only a few times every year to prevent high tides so the influence on low tide events will be limited. There is another interference of the Mo.S.E. system which may influence tidal flat ecosystems: a recent study performed by Tognin et al. (2021) shows that the Mo.S.E. system is likely to interfere with sedimentation processes on the Venice lagoon salt marshes. Reducing the tide level during storms, the gates closure prevents the flooding of marshes with sediment-rich waters, hence decreasing the sediment contribution vital to the marsh vertical accretion. The main sources of such sediments are tidal flats, from which wind waves resuspend large quantities of sediments during storms (Green & Coco, 2014), therefore we speculate that closures of the Mo.S.E. system gates may prevent the export of suspended sediments to the North Adriatic Sea, favoring the resedimentation within the lagoon and therefore also on tidal flats. Specific studies are needed in order to understand if such processes may alter the sedimentation/erosion processes of the studied tidal flat and therefore the fate of the *P. nobilis* population. Such effects may however be minor because the studied mudflat is located behind the Pellestrina barrier island, which protects the mudflat from the influence of the dominant winds, coming from NE and SE.

The use of a UAV system to detect *P. nobils* shells over a mudflat presents advantages and disadvantages with respect to field surveys. In this study, thanks to the ortho-photo mosaic produced from the UAV images, we could detect 5,252 shells, accurately locating them in a georeferenced system without provoking any perturbation of the system or damage to the shells. This result would have been impossible to obtain with a regular field survey. However, the method presents also important limits. Depending on the resolution of the ortho-photo, and in turn on the characteristics of the camera and the height of the flight, only shells larger than a certain size can be detected. The underestimation of juveniles' number and distribution may affect the study of population dynamics. However, we underline how in tidal systems the underestimation issue may, in general, also occur when performing field surveys. In fact, even when submerged by the tide, mudflats are characterized by very low water levels that make it difficult to swim or dive, especially when there is a highly dense *P. nobilis* population that colonizes the mudflat surface. Walking or diving in these conditions is dangerous and risks damaging the shells. Moreover, both aforementioned activities disturb the mudflat surface and suspend large amounts of sediments, thus preventing clear recognition of shells, particularly small ones. Even when the tide is low, walking between shells is difficult and produces perturbation and potentially damages the shells. In the case that the *P. nobilis* population develops within a dense seagrass meadow, the detection of small shells may also be impeded by leaves that cover them. Finally, if the purpose were the detection of the exact geographic location of each shell, as in our study, the use of a GNSS receiver would pose further difficulties considering the need to perform thousands of precise measurements. A second important limitation of the method based on UAV systems is the impossibility of distinguishing dead from alive/moribund *P. nobilis* individuals. This is a relatively minor problem when the large majority of individuals are alive and healthy, however, it may become an important issue if we consider the recent mortality events that have decimated the bivalve populations. In our case, pathogens have attacked the Venice lagoon populations several months after our survey, therefore our data describe the pre-epidemic condition of the studied *P. nobilis* population. Nevertheless, a reliable method for monitoring the mortality events would be highly desirable. Given the scale of the populations developing on tidal flats, as in our study site, field observations may not be the solution. A recent paper published by Cabanellas-Reboredo et al. (2019) found that shells might be affected by pathogens several weeks before showing the effects; hence, a simple observation of their state is not sufficient to determine their health condition. The uncertainty around the amount of time that the pathogens take to kill the individual does not allow a clear distinction between alive and healthy, and alive but moribund shells. Thus, posing a number of questions about the efficacy of field surveys for tracking the mortality events. Surveys performed using UAV systems may be able to provide a solution by using, e.g., thermal cameras as suggested by Franceschini et al. (2017) or other sensors/methods not yet explored.

Finally, our results are based on one single UAV flight, and no previous observations of the population distribution are available, therefore no conclusions on the temporal evolution of the system can be inferred. A comprehensive monitoring effort will be needed, at least yearly, to discriminate between dead and alive shells, monitor

the variations of the water quality parameters, record the morphological variations of the bottom topography, monitor the variation of the seagrass percentage cover and assess the possible influence of the Mo.S.E. system on the *P. nobilis* population.

6. Conclusions

The limits imposed on the survival of *P. nobilis* individuals by the number and duration of emersions is a key factor in the colonization of tidal systems. The population density patterns analyzed in our study show that above a certain topographic level, the frequency and duration of emersions are the main limiting factors for *P. nobilis* development and survival. Fewer individuals are recorded above this topographic level, where the risk of desiccation is high, while the majority of the population tends to colonize the mudflat depressions, where the number and frequency of emersions are low. In these deeper zones, the population densities range from low to high, which indicates that within a favorable environment there are other factors driving the observed density variability. Among such factors, the presence and percentage cover of the seagrass meadow is important, since we show that the dense *P. nobilis* population, with 0.8–2.68 N/m^2, grows within areas characterized by high-*C. nodosa* meadow cover (seagrass percentage cover >85%), and the density of the shells decreases with decreasing seagrass percentage cover. However, even considering both topography and seagrass cover as independent variables, we explain the majority but not the whole variability of the *P. nobilis* density. Therefore, there must be other factors driving the *P. nobilis* density patterns, probably linked to the availability of nutrients. In fact, we find that the bivalve tends to grow along the edge of the high-cover seagrass meadow that develops toward the main channel which connects to the inlet. We speculate that there is a trade-off between the advantage of being protected by the dense seagrass meadow and the interference that plants, trapping particles with their leaves and stems, may have with the *P. nobilis* filtering activity.

The presence and state of the seagrass meadows may also have had a role in the recolonization of *P. nobilis* of the Venice lagoon starting from 2006/2007. Maps and records show that the seagrass density and the extension of the meadows have increased over time, and the slight but constant increase of the water temperature during the last 18 years probably triggered this shift toward monospecific *C. nodosa* meadows. The presence of denser seagrass meadows has likely had a role in the decreased water turbidity that we have observed in the area, with positive feedback for the seagrasses and consequently for the colonization of *P. nobilis*.

The *P. nobilis* population of the Venice lagoon has been recently attacked by the pathogen *H. pinnae* as reported by the Centro Specialistico Ittico dell'Istituto Zooprofilattico Sperimentale delle Venezie (IZSVe; http://www.ismar.cnr.it/eventi-e-notizie/notizie/pinna-nobilis-si-aggrava-lemergenza). Given the current situation, our study can be considered as a pre-epidemic reference since the UAV survey was performed several months before the pathogens attacked the population. Since our research has detected some important geomorphological and environmental factors that drove the population growth over the last two decades, it provides management information for protection and/or restoration actions.

As for the use of UAV systems for monitoring *P. nobilis* within lagoon waters, we underline how this methodology allowed us to detect >5,000 individuals, thus building a georeferenced data set impossible to create with direct field observation methods. The method is extremely effective for the detection of standing shells, especially when a layer of water of 20–30 cm covers the seagrass meadow colonized by *P. nobilis*. On the contrary, when the tide is very low and the mudflat surface is emerged, the seagrass may cover the shells, especially in summer, producing errors in the estimation of their number and distribution. Therefore, very low tide conditions should be avoided to prevent the underestimation of the population. The two most important limitations of the method are the impossibility of distinguishing between alive and dead individuals and the underestimation of recruits and small individuals because, depending on the image resolution, only shells larger than a certain size are detectable. Such limits must be carefully considered when using UAV observations for modeling population dynamics.

Conflict of Interest

The authors declare no conflicts of interest relevant to this study.

Data Availability Statement

Data set for the article is freely available online in the Zenodo repository (DOI: https://doi.org/10.5281/zenodo.4812987). The UAV ortho-photo mosaic is freely available online in the Zenodo repository (DOI: https://doi.org/10.5281/zenodo.4812727). GIS databases and shape files on the distribution and abundance of seagrass species are freely available online in: (a) Atlante della Laguna (2021): website of the Venice Municipality on the Venice lagoon including seagrass maps and databases: http://cigno.atlantedellalaguna.it/maps/6/view (logged-in on 30 March 2021) and (b) SOLVe (2021): website of CORILA (Consorzio per il coordinamento delle ricerche inerenti al sistema lagunare di Venezia)—Database and maps of the observatory on the Venice Lagoon—Seagrass monitoring project: http://solve.corila.it/layers/?limit=20&offset=0&title__icontains=fanerogame (logged-in on 30 March 2021). Data collected using tide gauges and meteorological sensors by the Venice Municipality are freely available online on the website: https://www.comune.venezia.it/it/archivio/1653. Data collected with the multiparametric probe are available by request by contacting Ministero delle Infrastrutture e dei Trasporti—Provveditorato Interregionale alle OO.PP. del Veneto-Trentino Alto Adige-Friuli Venezia Giulia (httSp://provvedito-ratovenezia.mit.gov.it/).

References

Addis, P., Secci, M., Brundu, G., Manunza, A., Corrias, S., & Cau, A. (2009). Density, size structure, shell orientation and epibiontic colonization of the fan mussel *Pinna nobilis* L. 1758 (Mollusca: Bivalvia) in three contrasting habitats in an estuarine area of Sardinia (W Mediterranean). *Scientia Marina*, *73*(1), 143–152. https://doi.org/10.3989/scimar.2009.73n1143

Alomar, C., Vazquez-Luis, M., Magraner, K., Lozano, L., & Deudero, S. (2015). Evaluating stable isotopic signals in bivalve *Pinna nobilis* under different human pressures. *Journal of Experimental Marine Biology and Ecology*, *467*, 77–86. https://doi.org/10.1016/j.jembe.2015.03.006

Atlante della Laguna. (2021). *Website of the Venice Municipality on the Venice lagoon including seagrass maps and databases*. Retrieved from http://cigno.atlantedellalaguna.it/maps/6/view

Basso, L., Hendriks, I. E., & Duarte, C. M. (2015). Juvenile pen shells (*Pinna nobilis*) tolerate acidification but are vulnerable to warming. *Estuaries and Coasts*, *38*(6), 1976–1985. https://doi.org/10.1007/s12237-015-9948-0

Bowman, A. W., & Azzalini, A. (1997). *Applied smoothing techniques for data analysis*. Oxford University Press.

Cabanellas-Reboredo, M., Vázquez-Luis, M., Mourre, B., Álvarez, E., Deudero, S., Amores, Á., et al. (2019). Tracking a mass mortality outbreak of pen shell *Pinna nobilis* populations: A collaborative effort of scientists and citizens. *Scientific Reports*, *9*(1), 13355. https://doi.org/10.1038/s41598-019-49808-4

Cancemi, G., Buia, M. C., & Mazzella, L. (2002). Structure and growth dynamics of *Cymodocea nodosa* meadows. *Scientia Marina*, *66*(4), 365–373.

Carbognin, L., Teatini, P., & Tosi, L. (2004). Eustacy and land subsidence in the Venice Lagoon at the beginning of the new millennium. *Journal of Marine Systems*, *51*(1–4), 345–353. https://doi.org/10.1016/j.jmarsys.2004.05.021

Carella, F., Aceto, S., Pollaro, F., Miccio, A., Iaria, C., Carrasco, N., et al. (2019). A mycobacterial disease is associated with the silent mass mortality of the pen shell *Pinna nobilis* along the Tyrrhenian coastline of Italy. *Scientific Reports*, *9*(1), 2725. https://doi.org/10.1038/s41598-018-37217-y

Carella, F., Elisabetta, A., Simone, F., Fulvio, S., Daniela, M., Prado, P., et al. (2020). In the wake of the ongoing mass mortality events: Co-occurrence of Mycobacterium, Haplosporidium and other pathogens in *Pinna nobilis* collected in Italy and Spain (Mediterranean Sea). *Frontiers in Marine Science*, *7*, 48. https://doi.org/10.3389/fmars.2020.00048

Carniello, L., Defina, A., & D'Alpaos, L. (2009). Morphological evolution of the Venice lagoon: Evidence from the past and trend for the future. *Journal of Geophysical Research*, *114*, F04002. https://doi.org/10.1029/2008JF001157

Carniello, L., Silvestri, S., Marani, M., D'Alpaos, A., Volpe, V., & Defina, A. (2014). Sediment dynamics in shallow tidal basins: In situ observations, satellite retrievals, and numerical modeling in the Venice Lagoon. *Journal of Geophysical Research: Earth Surface 119*, 802–815. https://doi.org/10.1002/2013JF003015

Carr, J., D'odorico, P., McGlathery, K., & Wiberg, P. L. (2010). Stability and bistability of seagrass ecosystems in shallow coastal lagoons: Role of feedbacks with sediment resuspension and light attenuation. *Journal of Geophysical Research*, *115*, G03011. https://doi.org/10.1029/2009JG001103

Carrivick, J. L., Smith, M. W., & Quincey, D. J. (2016). Structure from motion in the geosciences. In *New analytical methods in Earth and environmental science*. Chichester: Wiley-Blackwell. https://doi.org/10.1002/9781118895818

Coma, R., Ribes, M., Serrano, E., Jiménez, E., Salat, J., & Pascual, J. (2009). Global warming-enhanced stratification and mass mortality events in the Mediterranean. *Proceedings of the National Academy of Sciences of the United States of America*, *106*(15), 6176–6181. https://doi.org/10.1073/pnas.0805801106

Coppa, S., de Lucia, G. A., Magni, P., Domenici, P., Antognarelli, F., Satta, A., & Cucco, A. (2013). The effect of hydrodynamics on shell orientation and population density of *Pinna nobilis* in the Gulf of Oristano (Sardinia, Italy). *Journal of Sea Research*, *76*, 201–210. https://doi.org/10.1016/j.seares.2012.09.007

Coppa, S., Quattrocchi, G., Cucco, A., de Lucia, G. A., Vencato, S., Camedda, A., et al. (2019). Self-organisation in striped seagrass meadows affects the distributional pattern of the sessile bivalve *Pinna nobilis*. *Scientific Reports*, *9*(1), 7220. https://doi.org/10.1038/s41598-019-43214-6

Cucchiaro, S., Cavalli, M., Vericat, D., Crema, S., Llena, M., Beinat, A., et al. (2018). Monitoring topographic changes through 4D-structure-from-motion photogrammetry: Application to a debris-flow channel. *Environmental Earth Sciences*, *77*(18), 632. https://doi.org/10.1007/s12665-018-7817-4

Cucchiaro, S., Straffelini, E., Chang, K. J., & Tarolli, P. (2021). Mapping vegetation-induced obstruction in agricultural ditches. *Agricultural Water Management*, *256*, 107083. https://doi.org/10.1016/j.agwat.2021.107083

Cucco, A., & Umgiesser, G. (2006). Modeling the Venice lagoon residence time. *Ecological Modelling*, *193*(1–2), 34–51. https://doi.org/10.1016/j.ecolmodel.2005.07.043

Curiel, D., Miotti, C., Checchin, E., Rismondo, A., Pierini, A., Zucchetta, M., et al. (2020). Distribuzione di Pinna nobilis Linnaeus, 1758 nella Laguna di Marano e Grado e nel settore a mare del Banco Mula di Muggia (Nord Adriatico). *Bollettino del Museo di Storia Naturale di Venezia*, *71*, 35–43.

Da Lio, C., Teatini, P., Strozzi, T., & Tosi, L. (2017). Computing the relative land subsidence at Venice, Italy, over the last fifty years. In *Managing cumulative risks through model-based processes* (pp. 999–1005).

D'Alpaos, L. (2010). *Fatti e misfatti di idraulica lagunare: La laguna di Venezia dalla diversione dei fiumi alle nuove opere alle bocche di porto*. Istituto veneto di scienze, lettere ed arti.

D'Alpaos, L., & Defina, A. (2007). Mathematical modeling of tidal hydrodynamics in shallow lagoons: A review of open issues and applications to the Venice lagoon. *Computers & Geosciences*, *33*(4), 476–496. https://doi.org/10.1016/j.cageo.2006.07.009

Ferla, M., Cordella, M., & Michielli, L. (2006). Aggiornamenti sulle osservazioni dei livelli di marea a Venezia. *Agenzia per la Protezione dell'Ambiente e per i servizi Tecnici. Rapporti*, *69*. Retrieved from https://www.isprambiente.gov.it/it/pubblicazioni/rapporti/aggiornamenti-sulle-osservazioni-dei-livelli-di

Folkard, A. M. (2005). Hydrodynamics of model *Posidonia oceanica* patches in shallow water. *Limnology & Oceanography*, *50*(5), 1592–1600. https://doi.org/10.4319/lo.2005.50.5.1592

Franceschini, G., Antonini, C., Bernarello, V., & Cacciatore, F. (2017). Applicazione di sistemi aeromobili a pilotaggio remoto (SAPR) a misure di densità in una colonia di *Pinna nobilis* (Linnaeus, 1758) nei dintorni di Chioggia (Laguna di Venezia, Bacino Sud): dati preliminari. In *Atti XLVIII Congresso SIBM* (Vol. 24, No. 1, p. 231).

Friedrichs, C. T., & Aubrey, D. G. (1988). Non-linear tidal distortion in shallow well-mixed estuaries: A synthesis. *Estuarine, Coastal and Shelf Science*, *27*, 521–545. https://doi.org/10.1016/0272-7714(88)90082-0

García-March, J. R., García-Carrascosa, A. M., & Pena, A. L. (2002). In situ measurement of *Pinna nobilis* shells for age and growth studies: A new device. *Ecology*, *23*(3), 207–217. https://doi.org/10.1046/j.1439-0485.2002.02781.x

García-March, J. R., Hernandis, S., Vázquez-Luis, M., Prado, P., Deudero, S., Vicente, N., & Tena-Medialdea, J. (2020). Age and growth of the endangered fan mussel *Pinna nobilis* in the western Mediterranean Sea. *Marine Environmental Research*, *153*, 104795. https://doi.org/10.1016/j.marenvres.2019.104795

García-March, J. R., Pérez-Rojas, L., & García-Carrascosa, A. M. (2007). Influence of hydrodynamic forces on population structure of *Pinna nobilis* L., 1758 (Mollusca: Bivalvia): The critical combination of drag force, water depth, shell size and orientation. *Journal of Experimental Marine Biology and Ecology*, *342*(2), 202–212. https://doi.org/10.1016/j.jembe.2006.09.007

García-March, J. R., & Vicente, N. (2006). Protocol to study and monitor *Pinna nobilis* populations within marine protected areas. In *MedPAN-Interreg IIIC-project. Malta Environment and Planning Authority (MEPA)*, 62. Retrieved from http://medpan.org/protocol-to-study-and-monitor-pinna-nobilis-populations-within-mpas/

Ghezzo, M., Sarretta, A., Sigovini, M., Guerzoni, S., Tagliapietra, D., & Umgiesser, G. (2011). Modeling the inter-annual variability of salinity in the lagoon of Venice in relation to the water framework directive typologies. *Ocean & Coastal Management*, *54*(9), 706–719. https://doi.org/10.1016/j.ocecoaman.2011.06.007

Gómez-Alba, J. A. S. (1988). *Guía de campo de los fósiles de España y de Europa* (pp. 925). Barcelona: Ediciones Omega S. A.

Green, M. O., & Coco, G. (2014). Review of wave-driven sediment resuspension and transport in estuaries. *Reviews of Geophysics*, *72*, 77–117. https://doi.org/10.1002/2013RG000437

Hendriks, I. E., Cabanellas-Reboredo, M., Bouma, T. J., Deudero, S., & Duarte, C. M. (2011). Seagrass meadows modify drag forces on the shell of the fan mussel *Pinna nobilis*. *Estuaries and Coasts*, *34*(1), 60–67. https://doi.org/10.1007/s12237-010-9309-y

Hendriks, I. E., Sintes, T., Bouma, T. J., & Duarte, C. M. (2008). Experimental assessment and modeling evaluation of the effects of the seagrass *Posidonia oceanica* on flow and particle trapping. *Marine Ecology Progress Series*, *356*, 163–173. https://doi.org/10.3354/meps07316

James, M. R., Chandler, J. H., Eltner, A., Fraser, C., Miller, P. E., Mills, J. P., et al. (2019). Guidelines on the use of structure from motion photogrammetry in geomorphic research. *Earth Surface Processes and Landforms*, *44*, 2081–2084. https://doi.org/10.1002/esp.4637

Kersting, D., Benabdi, M., Čižmek, H., Grau, A., Jimenez, C., Katsanevakis, S., et al. (2019). *Pinna nobilis: The IUCN Red List of Threatened Species 2019: e.T160075998A160081499*. RLTS.T160075998A160081499.en. https://doi.org/10.2305/IUCN.UK.2019-3

Kersting, D. K., Vázquez-Luis, M., Mourre, B., Belkhamssa, F. Z., Álvarez, E., Bakran-Petricioli, T., et al. (2020). Recruitment disruption and the role of unaffected populations for potential recovery after the *Pinna nobilis* mass mortality event. *Frontiers in Marine Science*, *7*, 594378. https://doi.org/10.3389/fmars.2020.594378

Koch, E. W., Ackerman, D. J., Verduin, J., & Van Keulen, M. (2006). Fluid Dynamic in seagrass ecology—From Molecules to ecosystem. In A. W. D. Larkum, R. J. Orth, & C. M. Duarte (Eds.), *Seagrasses: Biology, ecology, and conservation* (pp. 193–223). Dordeeht: Springer. https://doi.org/10.1007/978-1-4020-2983-7_8

Lee, K. S., Park, S. R., & Kim, Y. K. (2007). Effects of irradiance, temperature, and nutrients on growth dynamics of seagrasses: A review. *Journal of Experimental Marine Biology and Ecology*, *350*(1–2), 144–175. https://doi.org/10.1016/j.jembe.2007.06.016

Manca, E. (2010). *Effect of Posidonia oceanica* seagrass on nearshore waves and wave-induced flows [PhD Thesis] (p. 333). University of Southampton.

Manca, E., Cáceres, I. J. V. I., Alsina, J. M., Stratigaki, V., Townend, I., & Amos, C. L. (2012). Wave energy and wave-induced flow reduction by full-scale model *Posidonia oceanica* seagrass. *Continental Shelf Research*, *50*, 100–116. https://doi.org/10.1016/j.csr.2012.10.008

Marrocco, V., Sicuro, A., Zangaro, F., & Pinna, M. (2018). First record of the protected species *Pinna nobilis* (Linnaeus, 1758) in the Aquatina Lagoon (NATURA 2000 site IT9150003, South-East Italian coastline). *Nature Conservation*, *28*, 51. https://doi.org/10.3897/natureconservation.28.26112

Marrocco, V., Zangaro, F., Sicuro, A., & Pinna, M. (2019). A scaling down mapping of *Pinna nobilis* (Linnaeus, 1758) through the combination of scientific literature, NATURA 2000, grey literature and citizen science data. *Nature Conservation*, *33*, 21. https://doi.org/10.3897/natureconservation.33.30397

Matticchio, B., Carniello, L., Canesso, D., Ziggiotto, E., & Cordella, M. (2017). In L. D'Alpaos (Ed.), Recenti variazioni della propagazione della marea in laguna di Venezia: Effetti indotti dalle opere fisse alle bocche di Porto, Istituto Veneto di Scienze, Lettere ed Arti, Commissione di studio sui problemi di Venezia, Volume III: La laguna di Venezia e le nuove opere alle bocche (pp. 157–183).

McGlathery, K. J., Sundback, K., & Anderson, I. C. (2007). Eutrophication in shallow coastal bays and lagoons: The role of plants in the coastal filter. *Marine Ecology Progress Series*, *348*, 1–18. https://doi.org/10.3354/meps07132

Moriarty, D. J. W., & Boon, P. I. (1989). Interactions of seagrass with sediment and water. In A. W. D. Larkum, A. J. McComb, & S. A. Shepherd (Eds.), *Biology of seagrasses: A treatise on the biology of seagrass with special reference to the Australian region* (pp. 500–525). Amsterdam: Elsevier.

Old, G., Leeks, G., Cooper, D., McNeil, D., & Smith, P. (2001). *Two technological advances in continuous monitoring of suspended sediment transport and particle characteristics* [Technical report]. Wallingford, Oxon, UK: Centre for Ecology and Hydrology, Maclean Building, Crowmarsh Gifford.

Pawley, J. (Ed.) (2006). *Handbook of biological confocal microscopy* (Vol. 236). Springer Science & Business Media.

Prado, P., Andree, K. B., Trigos, S., Carrasco, N., Caiola, N., García-March, J. R., et al. (2020). Breeding, planktonic and settlement factors shape recruitment patterns of one of the last remaining major population of *Pinna nobilis* within Spanish waters. *Hydrobiologia*, *847*(3), 771–786. https://doi.org/10.1007/s10750-019-04137-5

Prado, P., Grau, A., Catanese, G., Cabanes, P., Carella, F., Fernández-Tejedor, M., et al. (2021). *Pinna nobilis* in suboptimal environments are more tolerant to disease but more vulnerable to severe weather phenomena. *Marine Environmental Research*, *163*, 105220. https://doi.org/10.1016/j.marenvres.2020.105220

Remondino, F., Nocerino, E., Toschi, I., & Menna, F. (2017). A critical review of automated photogrammetric processing of large datasets. International Archives of the *Photogrammetry, Remote Sensing & Spatial Information Sciences*, *42*, 591–599. https://doi.org/10.5194/isprs-archives-XLII-2-W5-591-2017

Rouanet, E., Trigos, S., & Vicente, N. (2015). From youth to death of old age: The 50-year story of a *Pinna nobilis* fan mussel population at Port-Cros island (Port-Cros National Park, Province, Mediterranean Sea). *Scientific Reports of the Port-Cros National Park*, *29*, 209–222.

Russo, P. (2012). Segnalazione di una grande colonia di *Pinna nobilis* (Linnaeus, 1758) nella Laguna di Venezia. *Notiziario SIM*, *30*(1), 31–34.

Sfriso, A., Facca, C., & Marcomini, A. (2005). Sedimentation rates and erosion processes in the lagoon of Venice. *Environment International*, *31*(7), 983–992.

Silvestri, S., D'Alpaos, A., Nordio, G., & Carniello, L. (2018). Anthropogenic modifications can significantly influence the local mean sea level and affect the survival of salt marshes in shallow tidal systems. *Journal of Geophysical Research: Earth Surface*, *123*, 996–1012. https://doi.org/10.1029/2017JF004503

Solidoro, C., Canu, D. M., Cucco, A., & Umgiesser, G. (2004a). A partition of the Venice Lagoon based on physical properties and analysis of general circulation. *Journal of Marine Systems*, *51*(1–4), 147–160. https://doi.org/10.1016/j.jmarsys.2004.05.010

Solidoro, C., Pastres, R., Cossarini, G., & Ciavatta, S. (2004b). Seasonal and spatial variability of water quality parameters in the lagoon of Venice. *Journal of Marine Systems*, *51*(1–4), 7–18. https://doi.org/10.1016/j.jmarsys.2004.05.024

SOLVe. (2021). *Website of CORILA (Consorzio per il coordinamento delle ricerche inerenti al sistema lagunare di Venezia)—Database and maps of the observatory on the Venice Lagoon—Seagrass monitoring project*. Retrieved from http://solve.corila.it/layers/?limit=20&offset=0&title__icontains=fanerogame

Tarolli, P., Sofia, G., & Dalla Fontana, G. (2012). Geomorphic features extraction from high-resolution topography: Landslide crowns and bank erosion. *Natural Hazards*, *61*, 65–83. https://doi.org/10.1007/s11069-010-9695-2

Tognin, D., D'Alpaos, A., Marani, M., & Carniello, L. (2021). Marsh resilience to sea-level rise reduced by storm-surge barriers in the Venice Lagoon. *Nature Geoscience*, *14*, 906–911. https://doi.org/10.1038/s41561-021-00853-7

Tosi, L., Teatini, P., & Strozzi, T. (2013). Natural versus anthropogenic subsidence of Venice. *Scientific Reports*, *3*(1), 2710. https://doi.org/10.1038/srep02710

Trigos, S., & Vicente, N. (2016). Transplantation protocol for the fan mussel *Pinna nobilis* in different types of substrate. *Marine Life*, *18*, 55–61.

Trincardi, F., Barbanti, A., Bastianini, M., Benetazzo, A., Cavaleri, L., Chiggiato, J., et al. (2016). The 1966 flooding of Venice: What time taught us for the future. *Oceanography*, *29*(4), 178–186. https://doi.org/10.5670/oceanog.2016.87

Viero, D. P., & Defina, A. (2016). Water age, exposure time, and local flushing time in semi-enclosed, tidal basins with negligible freshwater inflow. *Journal of Marine Systems*, *156*, 16–29. https://doi.org/10.1016/j.jmarsys.2015.11.006

Zavodnik, D., Hrs-Brenko, M., & Legac, M. (1991). Synopsis of the fan shell *Pinna nobilis* L. in the eastern Adriatic Sea. In F. Avon, & V. Gravez (Eds.), *Les Espèces Marines à Protéger en Méditerranée. Boudouresque C* (pp. 169–178). Marseille: GIS Posidonie Publ.